Research Article

Synthesis of MWCNT Forests with Alumina-Supported Fe$_2$O$_3$ Catalyst by Using a Floating Catalyst Chemical Vapor Deposition Technique

Shazia Shukrullah [iD],[1] **Muhammad Y. Naz** [iD],[1] **Norani M. Mohamed,**[2] **Khalid A. Ibrahim,**[3,4] **Abdul Ghaffar,**[1] **and Nasser M. AbdEl-Salam**[5]

[1]*Department of Physics, University of Agriculture, 38040 Faisalabad, Pakistan*
[2]*Department of Fundamental and Applied Sciences, Universiti Teknologi PETRONAS, 32610, Malaysia*
[3]*College of Engineering, Muzahimiyah Branch, King Saud University, Riyadh 11451, Saudi Arabia*
[4]*Department of Chemical Engineering, Al-Hussein Bin Talal University, Ma'an, Jordan*
[5]*Arriyadh Community College, King Saud University, 11437 Arriyadh, Saudi Arabia*

Correspondence should be addressed to Shazia Shukrullah; zshukrullah@gmail.com

In this study, multiwalled CNT bundles were synthesized with an alumina-supported Fe$_2$O$_3$ catalyst by using a floating catalyst chemical vapor deposition (FCCVD) technique. The metal catalyst was synthesized by dispersing Fe$_2$O$_3$ on alumina support. Ethylene molecules were decomposed over different amounts of metal nanoparticles in a FCCVD reactor. The CVD temperature was elevated from 600°C to 1000°C. The large active surface area of the metal nanobuds promoted the decomposition of a carbon precursor and the fast growth of CNT bundles. Least dense bundles of varying heights were observed at lower CVD temperatures of 600°C and 700°C. At 800°C, CVD process conditions were found suitable for the fast decomposition of hydrocarbon. The relatively better yield of well-structured CNTs was obtained with a catalyst weight of 0.3 g at 800°C. Above 800°C, CNT forests start losing alignment and height. The forest density was also decreased at temperatures above the optimum. The elemental composition of CNT bundles revealed the presence of carbon, aluminium, oxygen, and iron in percentages of 91%, 0.76%, 8.2%, and 0.04%, respectively. A very small I_D to I_G ratio of 0.22 was calculated for CNTs grown under optimized conditions.

1. Introduction

CNTs have been extensively researched for their unique physical and chemical traits. The characteristics like good electrical conductivity, mechanical strength, surface area, and chemical stability make CNTs an attractive material for high-end engineering devices [1–4]. In the past years, CNTs have been produced through arc discharge, laser ablation, fluidized bed CVD, fixed-bed CVD, plasma enhanced CVD, etc. [1–6]. Each one has its own merits and drawbacks. CVD is the most widely used method for the production of a high-carbon yield with selective growth. It is a relatively low-cost approach among the reported methods of synthesis of CNTs [5, 6]. During CVD synthesis of CNTs, a carbon precursor decomposes over a pure or mixed metal catalyst in a high-temperature environment. The released carbon diffuses into catalytic particles and recrystallizes on the catalyst surface in the form of nanotubes. The quality and quantity of the as-grown CNTs can be governed by manipulating the reaction parameters, such as the type of the carbon precursor, temperature, catalyst type, catalyst synthesis method, catalyst composition, particle size, and type of support [5, 6].

CVD-based synthesis of CNTs is a two-step process: preparation of the catalyst and the actual reaction for the nucleation of nanotubes. The nucleation step involves the dissociation of hydrocarbons over nanoparticles of a catalyst

supported by a transition metal or an inert powder (Al_2O_3, MgO, or SiO_2). A support to the catalyst is generally required to minimize the sintering of the metal catalyst, to enhance the mechanical strength of the catalyst, and to disperse the active phases of the catalyst. The metal catalysts are synthesized using the following techniques: sol-gel [7], metalloorganic CVD [8], impregnation [9], green synthesis, and coprecipitation [10]. A catalyst can also be synthesized in situ by decomposing the volatile metalloorganic compounds in a CVD reactor during the production of CNTs. The in situ synthesis of a catalyst is referred to as the floating catalyst CVD technique [11]. The nanosized powders of the metal catalysts have also been directly used to produce CNTs rather than through in situ synthesis [12].

Iron, nickel, and cobalt are the most commonly used metal catalysts for the CVD synthesis of CNTs. At higher temperatures, these metals exhibit high carbon solubility and diffusion and produce a better CNT yield. Also, having high melting points and low vapor pressures, these transition metals can drive a CVD process with a variety of carbon precursors even at lower temperatures. Other anticipated benefits of these metal catalysts include their strong adhesion with nanotubes as compared to other transition metal catalysts. These properties result in high process efficiency, narrow tube diameter, and high curvature of CNTs [13]. The solid organometallocenes are also being used to catalyze the CVD reaction. The materials include ferrocene, nickelocene, and cobaltocene. Since these catalysts release the nanoparticles of metals without requiring a support, the activity of the catalyst increases due to nanoparticles completely exposed by the carbon precursor. Generally, the tube diameter of CNTs can be controlled by optimizing the size of the catalyst particles [14, 15]. Other metal catalysts such as Al, Cu, Mg, Mn, Mo, Cr, Ag, Au, Sn, Pt, and Pd have also been reported to catalyze the decomposition of carbon precursors for CNT growth [16, 17]. Pirard et al. [18] deliberated on the kinetics of the MWCNT growth process in a fixed-bed CVD reactor with a horizontal tube alignment. A mixture of hydrocarbon, hydrogen, and helium was passed over an alumina-supported compound catalyst ($Fe\text{-}Co/Al_2O_3$). The decomposition of hydrocarbon did not happen without introducing a catalyst in the reaction. The activation energy of the CVD reaction was estimated at about $135 \, kJ \cdot mol^{-1}$. Sharif Zein et al. [19] synthesized MWCNTs by using a fluidized bed CVD technique. Ethylene was decomposed over an alumina-supported iron catalyst. Although the growth of MWCNTs without the use of a metal catalyst is possible in an arc-discharge technique, the mass production of relatively pure CNTs inevitably requires a metal catalyst in all well-known production techniques. The selection of an appropriate catalyst is perhaps the most significant step in the CNTs' growth process. The type of the catalyst explicitly determines the rate of decomposition of the carbon precursor, yield of CNTs, diameter distribution, and quality CNTs. Kathyayini et al. [20] conducted experiments on cobalt and iron catalysts under the same CVD process conditions. Considerably higher catalytic activity was observed with cobalt for the decomposition of acetylene under similar reaction conditions. Furthermore, the activity, carbon yield, and

growth parameters of a catalyst also varies with the type of carbon feedstock [21, 22]. To promote the catalytic activity in CVD-based processes, different catalyst supports are used to increase the active surface of the dispersed catalyst [23–25]. These supports include Al_2O_3, SiO_2, and MgO. In a catalyst-supported system, the catalyst-substrate interaction plays a crucial role in defining the morphology and structural properties of the catalyst and CNTs. Cheng et al. [26] synthesized wide and long ribbons and ropes of single-walled CNTs. A catalytic decomposition technique was used to produce CNT bundles of 100 mm diameter and 3 cm length. Ferrocene was vaporized and mixed with benzene, thiophene, and hydrogen. The mixture was carried into the reaction tube, the carbon precursor was catalytically decomposed, and MWCNT bundles were produced. The atomic iron was produced by reducing ferrocene with hydrogen gas. The iron particles were agglomerated into nanoparticles, which were used to decompose a carbon precursor for the production of CNTs. Delzeit et al. [27] grew MWCNT bundles on different substrates through a thermal CVD technique. An ion beam sputtering technique was used to prepare multilayered metal catalysts from Al, Fe, and Ni. The underlayers of Al were used as a support, whereas Fe and Ni were used as an active catalyst. The active catalyst was sputtered to form nanoparticles (<10 nm) on Al support. This Al-Fe combination supported the growth of CNTs in bundled form.

Usman et al. [28] synthesized aligned bundles of nitrogen-doped MWCNTs by using an aerosol-assisted CVD technique. Toluene and acetonitrile were nebulized to produce aligned MWCNTs with a ferrocene catalyst. The thermogravimetric analysis showed 3% to 6% ferrocene impurities in the final product. The bamboo-like structures of CNTs were improved further with an increase in nitrogen content. However, Raman and XRD analysis revealed the formation of structural defects with nitrogen doping. The ferrocene impurities existed in the form of Fe_2O_3, $a\text{-}Fe\text{-}Fe_3C$, and $g\text{-}Fe$. Yadav et al. [15] used a mixture of FcH and acetonitrile for the synthesis of nitrogen-doped nanotube bundles. However, impurity-free CNTs were reported in their work. Point et al. [29] used an electron cyclotron resonance-assisted CVD technique for the synthesis of CNT bundles. A mixture of ethanol, ferrocene, and benzylamine was thermally decomposed to produce CNT bundles [18]. The nitrogen concentration and CVD temperature showed good control over the structural properties of CNT bundles. The reported work was aimed at the production of MWCNT bundles by decomposing ethylene with the Fe_2O_3/Al_2O_3 catalyst. Alumina was used to support the metal catalyst and improve the chemical activity. It also serves as a base for the nucleation of CNTs. A floating catalyst CVD technique was used to produce CNTs with an alumina-supported catalyst by changing the CVD temperature from 600°C to 1000°C. The catalyst weight was varied from 0.1 g to 0.5 g, and CVD process time was fixed for 1 hour.

2. Materials and Methods

2.1. Synthesis of Metal Catalyst. All the chemicals were obtained from Sigma-Aldrich. A coprecipitation technique

was used to produce a metal catalyst by dispersing Fe_2O_3 over an alumina support. The composition of the catalyst was decided after a brief review of the published literature. The search of past literature reveals that the catalyst, formed from Fe_2O_3 and Al_2O_3 at a ratio of 6 to 4, is the best for the production of a better yield of good quality MWCNTs [30–32]. A similar mass ratio of the reactants was used to produce a metal catalyst. Aluminium nitrate ($Al(NO_3)_3 \cdot 9HO$) and iron nitrate ($Fe(NO_3)_3 \cdot 9H_2O$) were used as starting materials. The desired weights of both of iron and aluminium nitrates were dissolved separately in 3D water under constant stirring at 300 rpm. The stirring was carried out at room temperature. After 20 min of stirring, homogenous solutions of iron nitrate and aluminium nitrate were produced. Both solutions were mixed together and placed on a hotplate. Substantial stirring of the solution was carried out by maintaining the solution temperature at 80°C. An isothermal evaporation takes place under continuous stirring. The mixture was filtered, washed with distilled water, and heated in an oven for 12 hours at 100°C. The final product was ground into a powder of nano-sized particles. The average particle size remained in the range of 15 nm to 20 nm. The calcination of the catalyst powder was carried out in an electric furnace. The cabinet temperature was sustained at 650°C for 6 hours. The calcined catalyst was tested for its chemical composition, surface morphology, elemental distribution, and active sites.

2.2. Synthesis of Nanotubes. A horizontal FCCVD reactor was used to synthesize MWCNT bundles by decomposing ethylene molecules over an Fe_2O_3/Al_2O_3 catalyst. The effect of the process parameters, such as catalyst weight, process temperature, and process time, on the growth of CNT bundles was quantified using different characterization techniques. A FCCVD reactor (OTF-1200-80 mm) with a horizontal tube arrangement was used to produce CNT bundles. A schematic of the experimental setup is shown in Figure 1. It was composed of a splittable zone tube furnace with an 80 mm diameter quartz tube, which can achieve faster heating up to 1200°C and create a thermal gradient by adjusting the zone temperature. A precision temperature controller in the setup can provide 30 segments of heating and cooling steps with ±0.5°C accuracy. One end of the quartz tube was connected to a gas-mixing system where flowrates of argon, hydrogen, and ethylene gases were controlled by gas flowmeters. The other end of the tube was extended to the fume hood through a water channel. The ethylene was cracked over the Fe_2O_3/Al_2O_3 catalyst for nucleation of MWCNTs under the operating conditions summarized in Table 1.

The experiments were started with 0.1 g of catalyst. The catalyst was placed in a high-heating zone of the tube furnace. Argon gas was fed through the quartz tube at a flowrate of 250 sccm. The temperature of the reaction zone was elevated to 600°C at the rate of 15°C per minute. Once the chosen temperature was sustained, ethylene and hydrogen were also introduced into the quartz tube at flowrates of 100 sccm and 250 sccm, respectively. Ethylene and hydrogen were supplied for 60 min and the argon supply remained open even after the growth process was over. The furnace was allowed to cool down to ambient temperature under a continuous

supply of argon. Figure 2 shows the complete thermal profile of the heating cycle of the tube furnace for a CVD temperature of 800°C. After 12 hours of cooling, the argon supply was stopped and the carbon product was collected from the quartz tube. The collected samples were stored in glass containers and labeled according to the experiment conditions.

The synthesis process was first optimized for the CVD process temperature and then for the catalyst weight. The CVD temperature was varied from 600°C to 1000°C, and MWCNT bundles were produced by fixing the catalyst weight and process time at 1 g and 60 min, respectively. Once the optimum process temperature was identified, the catalyst weight was varied in the range of 0.1 to 0.5 g to identify the optimum value for the production of well-structured MWCNT bundles.

3. Results and Discussion

3.1. Characteristics of Metal Catalyst. During FCCVD synthesis of CNTs, decomposition of hydrocarbon and formation of CNT bundles were activated by the Fe_2O_3/Al_2O_3 catalyst. The ethylene molecules were dissociated catalytically on Fe_2O_3 nanoparticles, which were dispersed over Al_2O_3 support. On heating, Fe_2O_3 nanoparticles were reduced to pure metal and the free carbon diffused into the nanoparticles of the metal. The appearance of carbon density gradients, dissolved in metal nanoparticles, drove the carbon diffusion deep into the metal particles [30–32]. The diffused carbon precipitated out from the nanoparticles in the form of CNTs. To avoid dangling bonds, the carbon precipitated out from the least reactive facet of the catalyst particles for the formation of a nanotube.

In a CVD process, the growth of nanotubes is achieved through catalytic decomposition of hydrocarbons on a catalyst surface without the occurrence of spontaneous aerial pyrolysis [33]. The restriction of the gas pyrolysis to the surface of the catalyst can be controlled by deliberately selecting carbon sources, catalyst type, CVD reaction temperature, hydrocarbon flowrate, and catalyst weight. The catalyst of the given study was examined through scanning electron microscopy (SEM), energy dispersive X-ray spectroscopy (EDX), and mapping. SEM was used to study the morphology of the metal catalyst. The elements in the catalyst and their weight percentage were found using EDX analysis. Mapping images were also produced to detect the major elements in the catalyst composition and the dispersion of iron nanoparticles on the alumina support.

SEM micrographs of the surface of the metal catalyst are shown in Figure 3. FESEM micrographs confirmed the growth of Fe_2O_3 nanoparticles on Al_2O_3 support. The magnified FESEM micrograph revealed that the nanoparticles were almost of the same size. The particle size was measured in the range of 15 nm to 20 nm. These nanobuds and other active sites on the alumina support promoted the activity of the Fe_2O_3 catalyst. The hydrocarbon quickly decomposed by releasing carbon, which precipitated out in the form of nanotubes at lower activation energies. The nanobuds gave a large active surface area, which was favorable for the fast growth of CNT bundles. The rough surface of the alumina support was
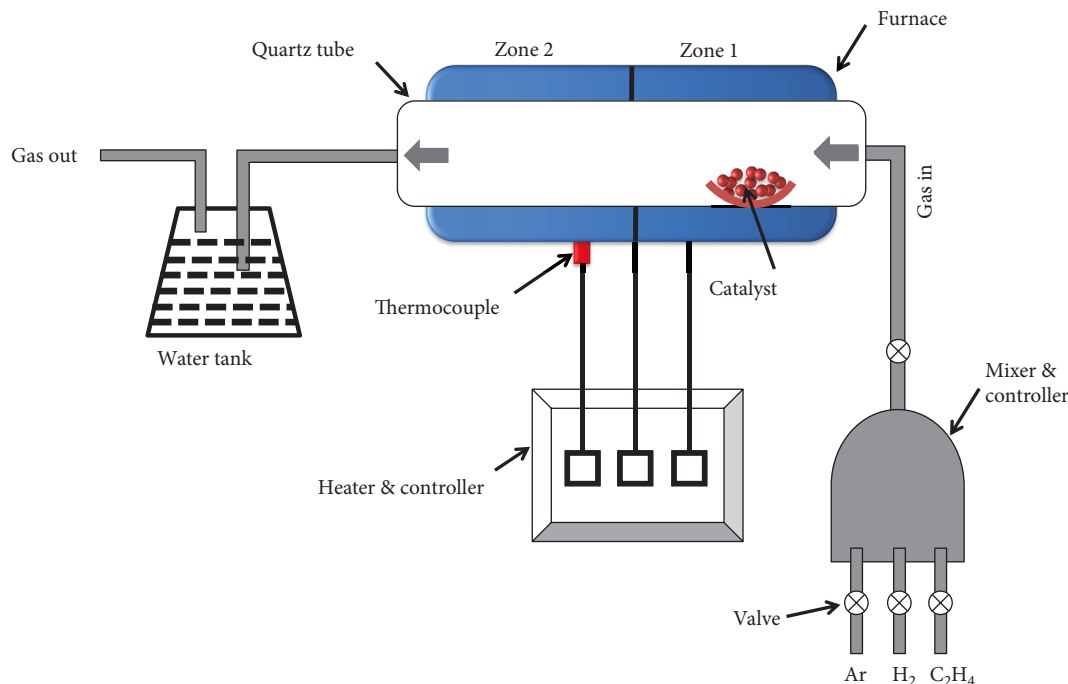
FIGURE 1: Schematic of the FCCVD reactor for the production of CNT bundles.

TABLE 1: Process parameters for CVD synthesis of MWCNT bundles.

Process	Variation
Weight of the catalyst	0.1 to 0.5 g
CVD process time	60 min
CVD process temperature	600 to 1000°C
Ethylene flowrate	100 sccm
Argon flowrate	250 sccm
Hydrogen flowrate	250 sccm
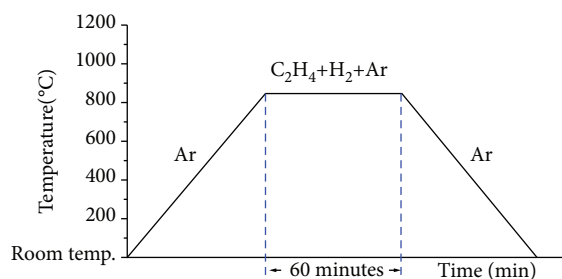
FIGURE 2: A typical temperature profile of the horizontal FCCVD process.
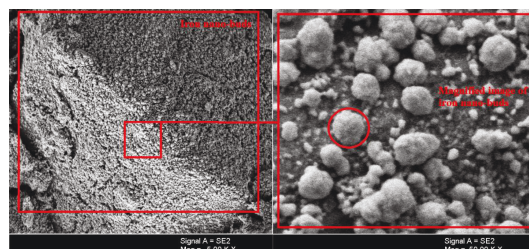

FIGURE 3: FESEM illustration of the catalyst of mixed metal oxides.

which possesses both acidic and basic groups. Therefore, during the synthesis of CNTs, the reaction kinetics follows the path requiring minimum energy for the initiation of the nucleation of CNTs.

The elemental composition and relative weight percent of the catalyst components was studied by generating the EDX spectrum. EDX analysis is based on the X-ray spectrum, which is generated by bombarding the sample with a focused beam of electrons. This analysis provides a localized chemical composition of the sample. An EDX spectrum of the catalyst of mixed metal oxides is shown in Figure 4. The major elements and their concentration at a specific point on the catalyst are given in Table 2. The catalyst was composed of iron, oxygen, and aluminium. The weight of these elements was measured at about 33.81%, 21.70%, and 44.49%, respectively. These findings infer the formation of metal oxide in the catalyst.

Elemental mapping of the as-synthesized catalyst was carried out at a microstructural level with a FESEM-based EDX technique. The elemental maps can be used in displaying the distribution of elements in the textural context,

also supportive of the strong interactions between gases and solids, even at lower activation energies, for nucleation of nanotubes [34]. Hussein et al. [35] reported that the use of mixed metal oxides is not only attractive as a catalyst, but as a catalyst support as well. In such catalysts, good dispersion of catalyst particles over stable support is expected,
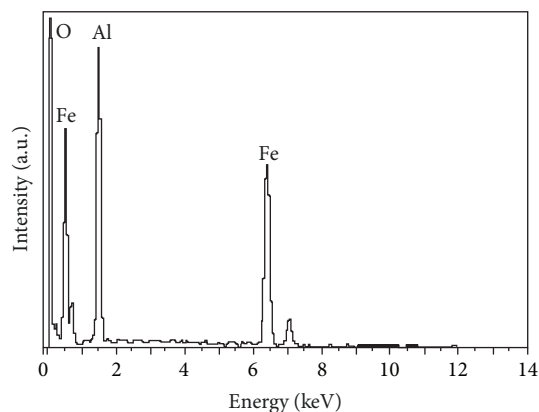
Figure 4: EDX spectrum of the catalyst of mixed metal oxides.

Table 2: Elemental composition of the catalyst of mixed metal oxides.

Element	Weight%	Atomic%
Oxygen	33.81	54.76
Iron	44.48	26.94
Aluminium	21.71	18.30
Total	100	100

particularly for showing compositional zonation. The maps of the catalyst provided the spatial distribution of the elements throughout the catalyst. The mapping images of the tested catalyst are shown in Figure 5. These images show that the catalyst is formed of O, Al, and Fe in the catalyst. Furthermore, the images also confirm that iron species are uniformly dispersed on the alumina surface. The uniformly dispersed iron with high concentration, as observed in EDX analysis and elemental mapping, is supportive of the high yield of CNT bundles. Kouravelou and Sotirchos [36] tested two compositions of the Fe_2O_3/Al_2O_3 catalyst for the production of CNTs. It was reported that both compositions are equivalent with respect to the rate of decomposition of the carbon precursor. However, a better carbon yield was possible with the catalyst having a high concentration of Fe_2O_3. Abad et al. [37] and Kierzkowska et al. [38] revealed that the Fe_2O_3/Al_2O_3 catalyst with a high wt.% of Fe_2O_3 exhibits high catalytic activity and promotes the decomposition of the hydrocarbons.

Alumina is a better catalyst support than other metallic materials. It provides support for the high dispersion of metal nanoparticles and density of active sites [33, 39]. Chemical interactions between the Al_2O_3 support and the metal catalyst expedite the oxidation process taking place at the interface of the metal catalyst and Al_2O_3 support [40]. Alexiadis and Verykios [31] revealed that a strong interaction between the catalyst and support phases is important for both the quality and quantity of CNTs. Both materials are equally important and effectively participate in a CVD reaction for the nucleation of CNTs. Mattevi et al. [41] preferred alumina over silica and other similar kinds of materials for catalyst support. Recent in situ analyses of the production of CNTs

with different carbon sources and catalysts have also strengthened the claim of Mattevi et al. [41]. Nevertheless, a study by Noda et al. [42] reported that the oxide substrates are more likely used for physical support to the metal catalyst; however, they can play some chemical roles in the nucleation of CNTs. Contrarily, Kumar and Ando [43] emphasized more on the structure and chemical state of the support than the type of metal. Zhao et al. [44] suggested that although CNTs can be produced with mixed metal oxides having lower iron oxide content, it is difficult to increase the growth rate, yield, and length of nanotubes without increasing the iron content in the catalyst. They concluded that if the iron content of the catalyst is high, more and more catalyst particles will act as "seeds" for the nucleation of CNTs at a fast rate.

Tessonnier and Su [45] deduced a crystallographic relationship between catalyst particles and the number of carbon layers for the CVD growth of nanotubes. Since high CVD temperatures are maintained to ensure the crystalline growth of nanotubes, the carbon source should be such that it does not thermally decompose into amorphous carbon at a high temperature. The amorphous carbon poisons the metal particles by reducing their catalytic activity. Under optimized CVD conditions, the mixed metal oxides promote the growth rate of CNTs and prevent catalyst particles from deactivating by removing the carbon from the surface of the catalyst. If a CVD process is carried out at temperatures exceeding the optimum, thermal degradation of the catalyst can happen either due to the formation of active phase crystallites or due to a collapse of the pore structures of the support. The collapse of solid-state reactions of the active phase of the catalyst with support is also possible at very high CVD temperatures.

3.2. Characteristics of Bundled CNTs. The nucleation of nanotubes happens in three steps, namely, cap nucleation, cap lift-off, and tube lengthening. The poisoning of the catalyst affects the length and purity of CNTs. It is detrimental to the CNTs' growth process. It prevents the carbon precursor from accessing the catalyst, and consequently, it prevents the cap lift-off and growth of nanotubes. The optimized CVD temperature helps in minimizing the poisoning and encapsulation of the catalyst particles during nucleation of CNTs. The most common growth mechanism of carbon filaments is the catalytic decomposition of the precursor and bulk carbon diffusion into the catalyst particles [46, 47]. The precursor molecules decompose and release carbon and hydrogen at the frontally exposed surface of the catalyst. The active carbon atoms dissolve and diffuse into the catalyst and precipitate at its trailing end in the form of nanotubes. Since the catalyst particles were having high thermal conductivity, the exothermic decomposition of ethylene may generate some temperature gradients across the particle by increasing the process temperature. Since the solubility/diffusion of carbon atoms in the catalyst is temperature dependent, the high precipitation of carbon into nanotubes takes place in the low temperature zones of the catalyst.

The formation and length of CNTs are driven by the carbon concentration gradients across the catalyst. CNTs
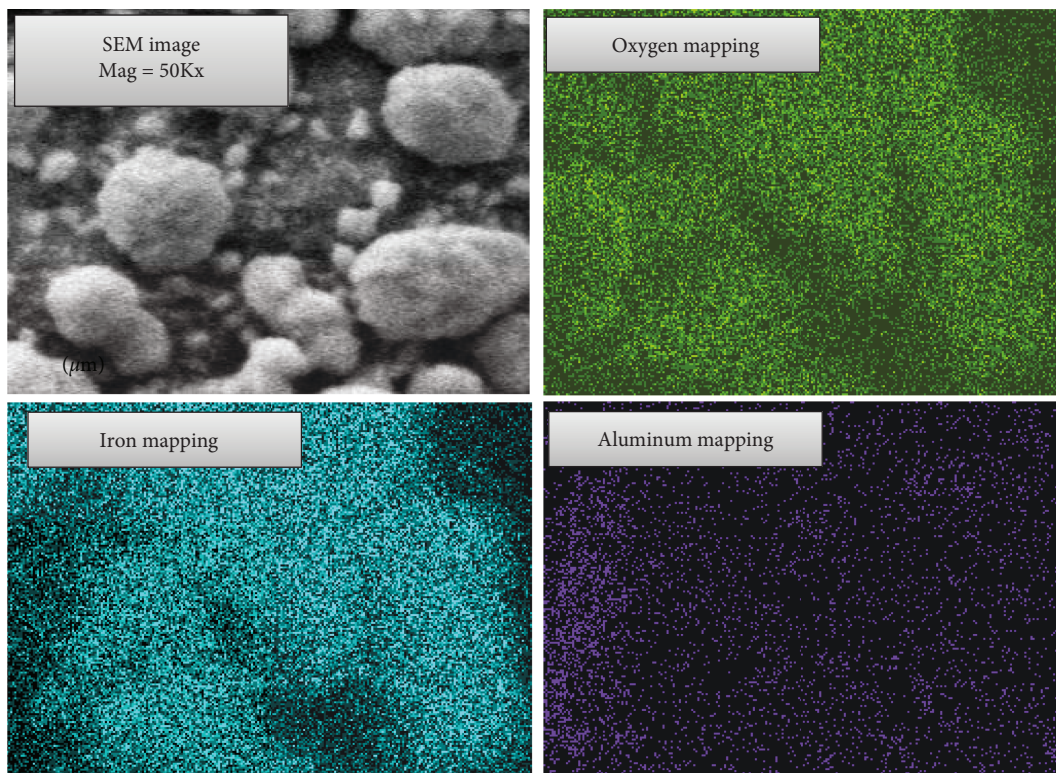
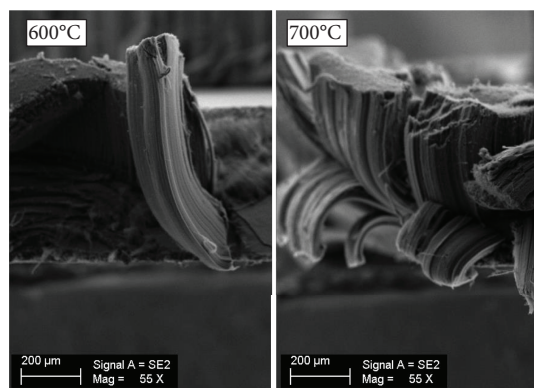FIGURE 5: Elemental maps of the catalyst of mixed metal oxides.

FIGURE 6: SEM micrographs of MWCNT bundles synthesized at 600°C and 700°C CVD temperatures.

FIGURE 7: SEM micrographs of MWCNT bundles synthesized at a CVD temperature of 800°C.

keep on growing unless the leading face of the catalyst is poisoned by the amorphous carbon. At this point, the CNT forest stops growing and the continuing CVD process adds impurities to the product. The denseness and height of the forest also depends on the CVD temperature. In this study, the effect of the CVD temperature on CNT parameters was examined in the range of 600°C to 1000°C by fixing the catalyst weight at 0.3 g. The least dense bundles of different heights were obtained at 600°C and 700°C CVD temperatures. As shown in Figure 6, very few CNT bundles grow at 600°C. At 700°C, the growth of CNTs was increased and several CNT bundles of varying lengths and directions were seen in SEM micrographs. At these temperatures, the catalyst
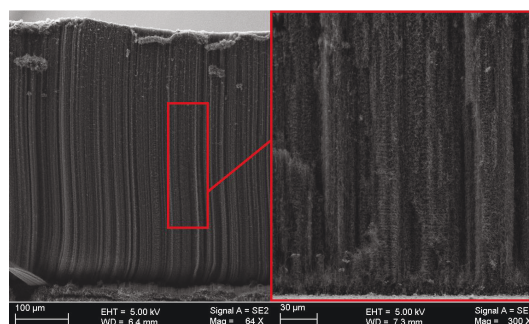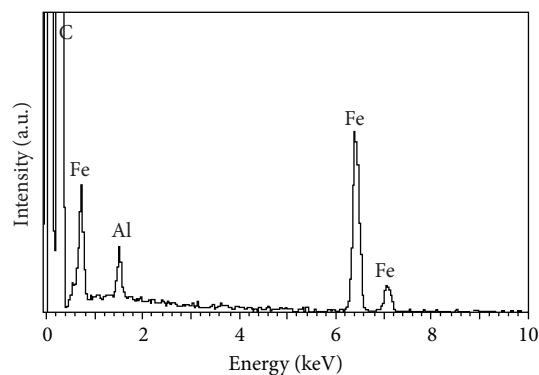

FIGURE 8: EDX spectrum of MWCNT bundles grown at a CVD temperature of 800°C.
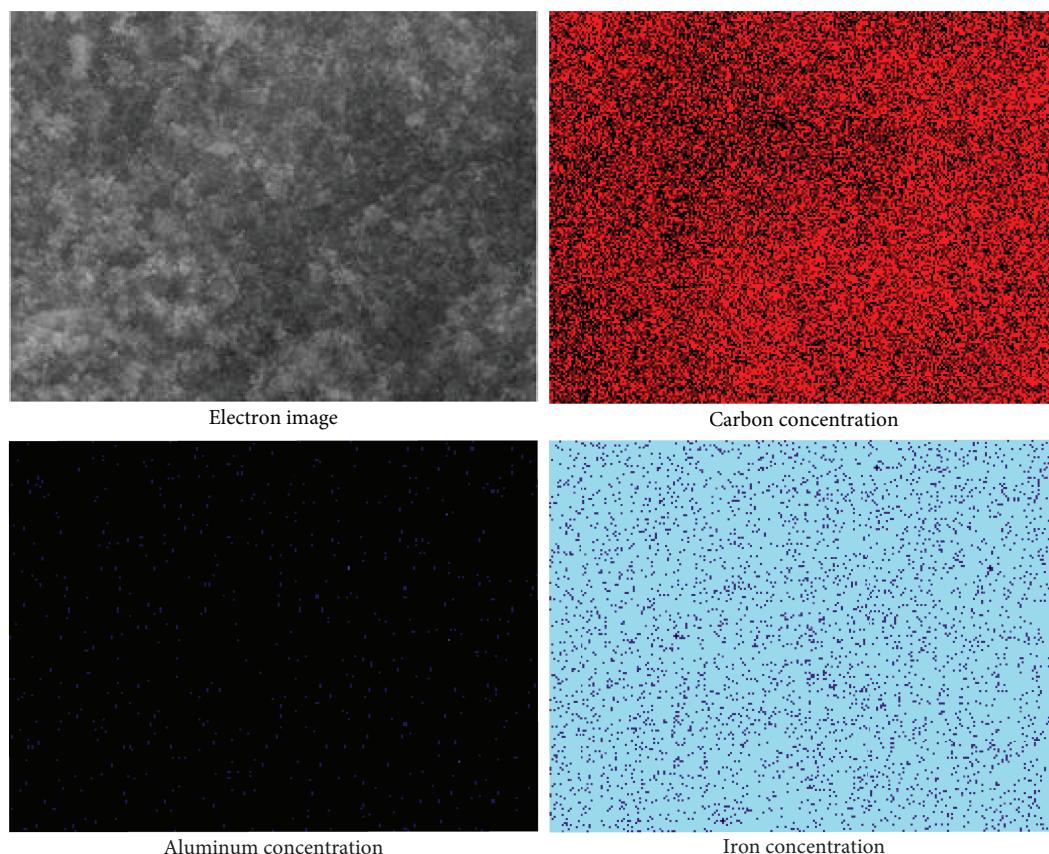
FIGURE 9: Mapping of MWCNT bundles grown at a CVD temperature of 800°C.

might not have fully activated and/or the decomposition of hydrocarbon molecules did not take place at the rate required for a dense and aligned growth of the CNT forest [48]. With a further increase in temperature, CVD conditions became suitable for the fast decomposition of hydrocarbon. At a CVD temperature of 800°C, the catalytic activity of the metal catalyst was appreciably increased. As shown in Figure 7, the dense and aligned growth of the CNT forest was noticed at this temperature. The quantity and quality of CNTs were also improved by increasing the CVD temperature. The smooth growth of CNT assemblies of the same height was seen in SEM micrographs.

With a further increase in CVD temperature above 800°C, CNT bundles start losing their alignment and height. The forest density was also decreased at temperatures above the optimum. CNTs were making upwardly growing vines that were intertwining with each other in the form of loose bundles. The scattered diameter distribution of CNT bundles was observed at temperatures above and below the optimum. The imbalanced rate of decomposition of hydrocarbon molecules and the rate of carbon diffusion into the catalyst particles promoted the formation of amorphous carbon [49]. At a high CVD temperature, the aggressive diffusion and precipitation of carbon into nanotubes raise the impurity level of the product [50].

The elemental composition of the as-grown CNT bundles was measured using EDX. A typical EDX spectrum of CNTs is shown in Figure 8. Carbon, aluminium, oxygen, and ferric contents were detected in the EDX spectrum with their weight percentages of 91%, 0.76%, 8.2%, and 0.04%, respectively. Carbon was detected with the highest wt.%, whereas the other three elements existed in fractional amounts. The carbon content exhibited an increase, while aluminium, oxygen, and ferric contents were decreased by increasing the CVD temperature from 600°C up to the optimum.

The growth of CNTs in bundles is attributed to the Al_2O_3 support, which promoted the Van der Waals forces whereby the degree of crystallization and handling of CNTs was increased [51]. The iron buds on the Al_2O_3 support were having unfilled d-shells; therefore, they exhibited better catalytic activity. The embedded buds worked as a seed for the growth of CNT bundles. Figure 9 reports the composition of CNT bundles in the form of elemental maps. These maps were generated using the mapping tool of the FESEM setup. At low CVD temperatures, the carbon product contained many unreacted catalyst particles. The appearance of a high concentration of aluminium and iron in elemental maps at lower CVD temperatures reveals the low activity of the catalyst. The highest carbon concentration was observed under the optimized CVD temperature. The aluminium content was almost negligible, whereas very few traces of iron were observed in the maps, as shown in Figure 9. These results were in line with the elemental composition predicted with EDX analysis.

(a) CNTs grown at a CVD temperature of 600°C

(b) CNTs grown at a CVD temperature of 700°C

(c) CNTs grown at a CVD temperature of 800°C

(d) CNTs grown at a CVD temperature of 900°C

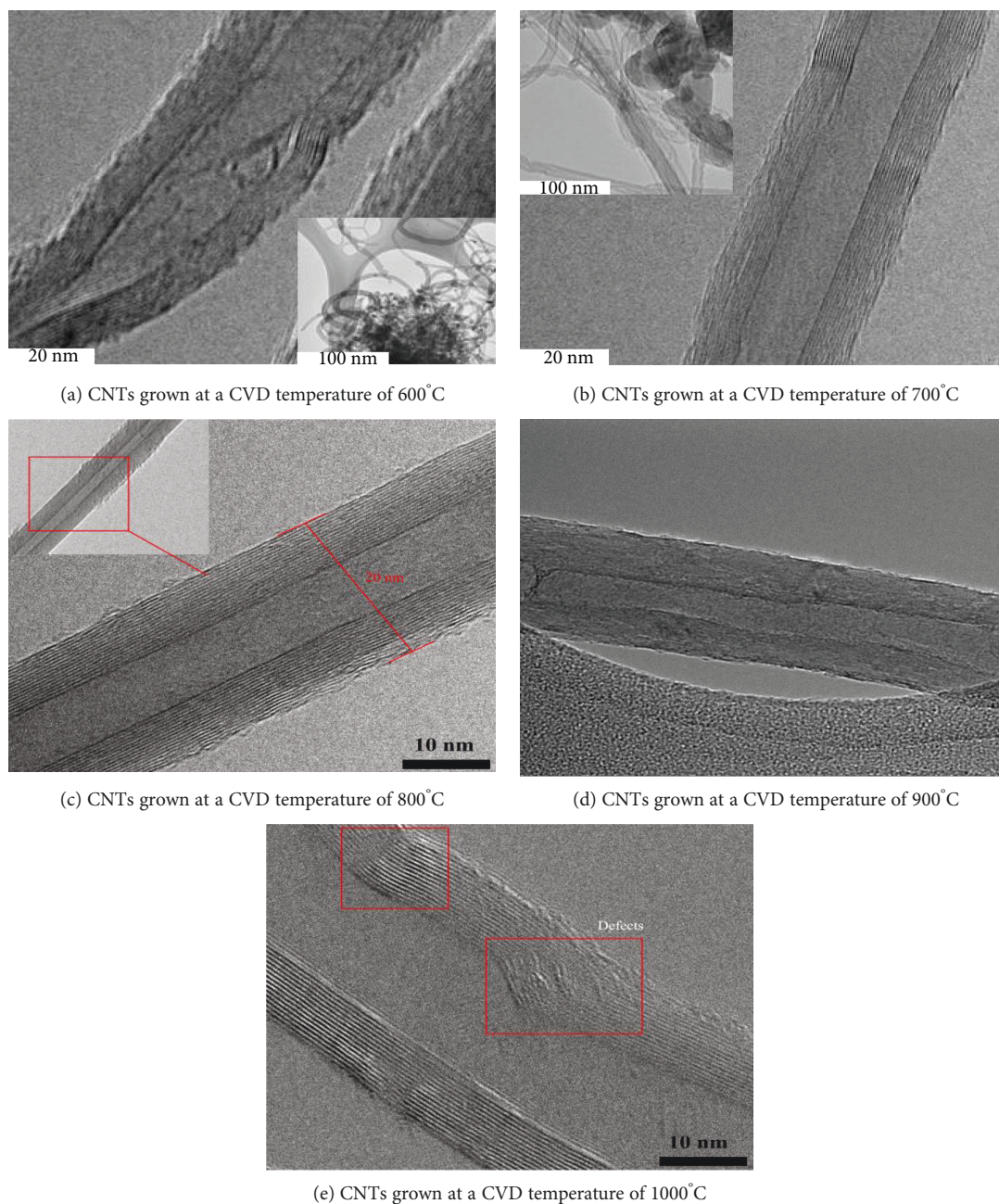(e) CNTs grown at a CVD temperature of 1000°C

FIGURE 10: TEM micrographs of MWCNT bundles synthesized at different CVD temperatures by using the 0.3 g catalyst.

The internal structure of individual nanotubes was examined using the TEM technique. TEM images, as shown in Figure 10, confirmed the formation of multiwalled CNT structures. The length, inner diameter, outer diameter, interlayer spacing, and number of walls of as-grown nanotubes were changed with a change in CVD temperature. The outer diameter was measured in the range of 20 nm to 30 nm. At the optimized temperature, the interlayer spacing was measured at about 0.33 nm. This spacing is in good agreement with the interplanar spacing of graphite. The narrow diameter distribution range and close matching of the interlayer spacing with graphite reflects the well-structured growth of CNTs. The structural defects and interlayer spacing changed

with a change in the CVD temperature and catalyst weight. A change in structural parameters might be due to a shift in the curvature of the graphene sheet with CVD temperature.

Kharissova and Kharisov [52] reported a change in the interlayer spacing with tube diameter and thickness. The tube diameter increased slightly at temperatures above the optimum. A SAED pattern of CNTs, grown at the optimized CVD temperature, is shown in Figure 11. Several continuous diffraction rings were observed in the SAED pattern. The high brightness of the diffraction rings reflects the polycrystalline nature of CNT structures and the absence of amorphous traces from the sample. The crystal planes (100) and (110) of graphite symmetry formed the inner and outer
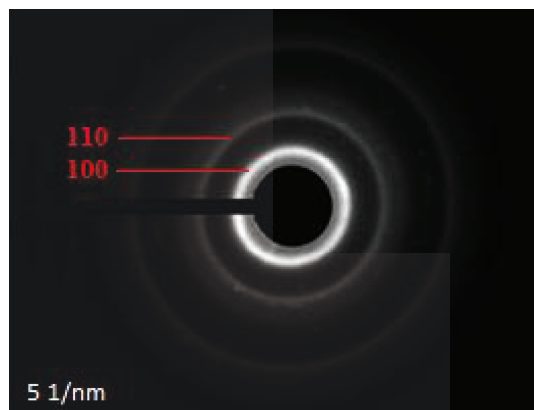
FIGURE 11: SAED pattern of MWCNT bundles synthesized at a CVD temperature of 800°C.
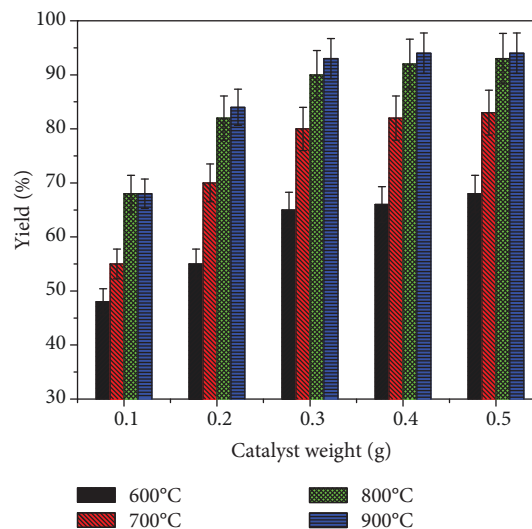

FIGURE 12: Carbon yield versus catalyst weight at different CVD temperatures.

FIGURE 13: Carbon yield versus catalyst weight at a CVD temperature of 800°C.

bright rings, respectively. Such Miller indices indicate the hexagonal structure of carbon crystals. However, the sharpness of graphite reflections was slightly diffused at temperatures other than the optimum.

The effect of catalyst weight on CNT structures was also investigated at different CVD temperatures. For smaller catalyst weights, low-slung CNTs were formed. Least dense forests of CNT bundles of varying lengths and directions were seen. Nanotubes intertwined with each other in the form of loose bundles. Some carbon soot was also noticed in the sample showing an insufficient amount of the catalyst to engage the carbon released during ethylene cracking. The height, alignment, and density of the forest also remained low due to catalyst poising. For 0.3 g of catalyst, the yield and quality of the CNT networks remarkably improved. Very few traces of amorphous carbon were seen in the sample.

Similar results were obtained with the 0.4 g catalyst except for some unreacted catalyst in the sample. Some of the CNT bundles were entangled, especially along the boundary of the main forest. For the 0.5 g catalyst, the forest growth was not as smooth as observed with the 0.3 g catalyst. An extra carbon-rich environment was required to utilize the larger catalyst amounts and to maintain the homogeneity of the reaction. Furthermore, a high process temperature would be required for the fast decomposition of the precursor molecules. The large supply of precursor molecules and the high process temperature may make a CVD process more complex, especially during the scale-up stage [53]. Also, an increase in catalyst weight above the optimum did not raise the carbon yield at the same rate [54]. Figure 12 depicts the percentage yield of the carbon obtained by changing the catalyst weight at different CVD temperatures. The percentage yield did not increase appreciably beyond 0.3 g of catalyst. The carbon yield increases with temperature from 600°C to 000°C; thereafter, it reaches a steady state. Figure 13 shows that under optimized temperature and catalyst weight conditions, the percentage yield was measured at about 93%.

Raman spectroscopy was used to analyze the crystallinity of the CNT structures. Figure 14 shows the Raman spectra of the CNT bundle growth with the 0.3 g catalyst at different CVD temperatures. The ratio of intensities of defective and graphitic bands was used as an indicator of the crystallinity of CNT structures. In a Raman spectrum, the intensity of the D-band corresponds to the defects in the CNT structures and the intensity of G-band reflects the crystalline nature of the CNT structures [6]. In the reported Raman spectra, G-bands existed in the range of 1600-1610 cm^{-1}. This range of Raman shift corresponds to the sp^2 hybridization of carbon-carbon bonds responsible for the formation of CNT structures. The sp^2 hybridized carbon bonds reveal in-plane stretching of graphene sheets and high crystallinity of the structures. The Raman shift for D-bands was measured at about ~1360 cm^{-1}, which corresponds to the sp^3-hybridizaton of carbon-carbon bonds. The sp^3 hybridized bonding of carbon atoms in CNTs reflects the presence of impurities and defects in their structures. Very small I_D to I_G ratio of 0.22 was calculated for CNTs grown under optimized conditions. For all the temperatures and catalyst weights other
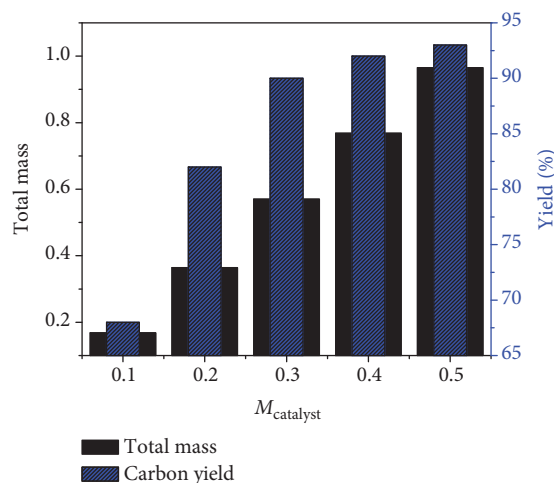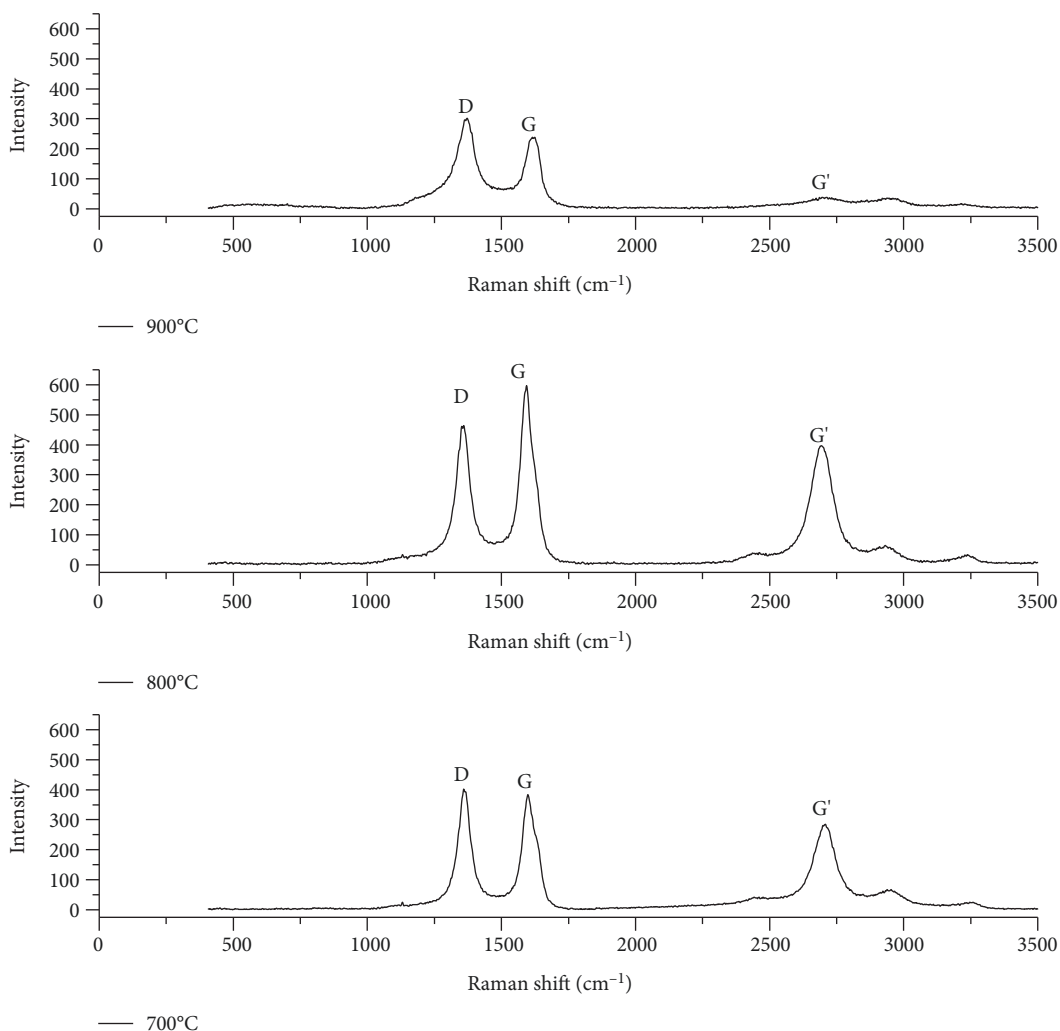
FIGURE 14: Raman spectra of MWCNT bundles produced at different CVD temperatures.

than the optimized ones, the I_D/I_G ratio remained significantly higher by showing the presence of structural defects and impurities in the product.

4. Conclusions

The forests of MWCNTs were grown through a FCCVD technique by decomposing ethylene molecules over an alumina-supported Fe_2O_3 catalyst. A coprecipitation technique was used to disperse iron oxide over an alumina support for the synthesis of the Fe_2O_3/Al_2O_3 catalyst. The particle size was measured in the range of 15 nm to 20 nm. The catalyst was composed of iron, oxygen, and aluminium. The weight of these elements was measured at about 33.81%, 21.70%, and 44.49%, respectively. The nanobuds of Fe_2O_3 and other active sites on the alumina support promoted the catalytic activity of the catalyst for the fast nucleation of nanotubes. The nanobuds gave a large active surface area, which was favorable for fast growth of CNT bundles. A relatively better yield of well-structured CNTs was obtained with a catalyst weight of 0.3 g at a CVD temperature of 800°C. The least dense bundles of different heights were observed at CVD temperatures of 600°C and 700°C. At 800°C, CVD conditions became suitable for the fast decomposition of hydrocarbon. A denser and aligned growth of the CNT forest was noticed at this temperature. The yield and structural quality of the nanotubes was also increased with the rise in CVD temperature, and with the further increase in CVD temperature above 800°C, CNT bundles start losing their alignment and height. The forest density was also decreased at temperatures above the optimum. CNTs were making upwardly growing vines that were intertwining with each other in the form of loose bundles. The elemental composition of CNT bundles revealed the presence of carbon, aluminium, oxygen, and ferric contents in the percentage of 91%, 0.76%, 8.2%, and 0.04%, respectively. The sp^2 hybridized carbon bonds in CNTs revealed the in-plane stretching of graphene sheets and the high crystallinity of the structures. The minimum I_D/I_G ratio of 0.22 was calculated for CNTs grown under optimized conditions. For all the temperatures and catalyst weights other than the optimized ones, the I_D/I_G ratio remained significantly higher by showing the presence of structural defects and impurities in the product.

Data Availability

There is no restriction on the presented data. The authors can provide all the data on request.

Conflicts of Interest

The authors declare that there is no conflict of interest regarding the publication of this paper.
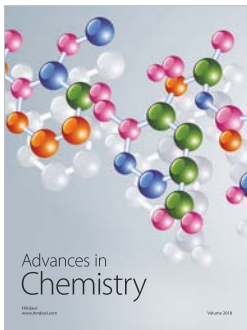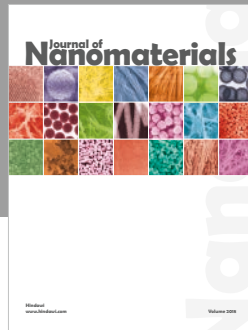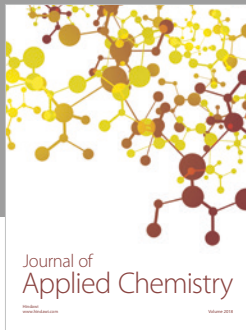
Acknowledgments

References

[1] L. C. Qin, "Electron diffraction from carbon nanotubes," *Reports on Progress in Physics*, vol. 69, no. 10, pp. 2761–2821, 2006.

[2] S. Iijima, "Helical microtubules of graphitic carbon," *Nature*, vol. 354, no. 6348, pp. 56–58, 1991.

[3] K. B. K. Teo, C. Singh, M. Chhowalla, and W. I. Milne, "Catalytic synthesis of carbon nanotubes and nanofibers," *Encyclopedia of Nanoscience and Nanotechnology*, vol. 1, pp. 665–686, 2004.

[4] C. H. Su, C. R. Lin, C. H. Hung, C. Y. Chang, and L. Stobinski, "Novel process to synthesize the well-size-controlled carbon nanotubes using Fe/TiO_2 as catalyst by sol-gel method," *Surface and Coatings Technology*, vol. 200, no. 10, pp. 3211–3214, 2006.

[5] A. Gangele, C. S. Sharma, and A. K. Pandey, "Synthesis of patterned vertically aligned carbon nanotubes by PECVD using different growth techniques: a review," *Journal of Nanoscience and Nanotechnology*, vol. 17, no. 4, pp. 2256–2273, 2017.

[6] S. Shukrullah, N. M. Mohamed, Y. Khan, M. Y. Naz, A. Ghaffar, and I. Ahmad, "Effect of gas flowrate on nucleation mechanism of MWCNTs for a compound catalyst," *Journal of Nanomaterials*, vol. 2017, Article ID 3407352, 9 pages, 2017.

[7] C. R. Lin, C. H. Su, C. H. Hung, C. Y. Chang, and L. Stobinski, "Characterization of bamboo-like CNTs prepared using sol-gel catalyst," *Diamond and Related Materials*, vol. 14, no. 3-7, pp. 794–797, 2005.

[8] C. Xu and J. Zhu, "One-step preparation of highly dispersed metal-supported catalysts by fluidized-bed MOCVD for carbon nanotube synthesis," *Nanotechnology*, vol. 15, no. 11, pp. 1671–1681, 2004.

[9] V. Ivanov, J. B. Nagy, P. Lambin et al., "The study of carbon nanotubules produced by catalytic method," *Chemical Physics Letters*, vol. 223, no. 4, pp. 329–335, 1994.

[10] J. A. Schwarz, C. Contescu, and A. Contescu, "Methods for preparation of catalytic materials," *Chemical Reviews*, vol. 95, no. 3, pp. 477–510, 1995.

[11] P. Nikolaev, M. J. Bronikowski, R. K. Bradley et al., "Gas-phase catalytic growth of single-walled carbon nanotubes from carbon monoxide," *Chemical Physics Letters*, vol. 313, no. 1-2, pp. 91–97, 1999.

[12] Y. Wang, F. Wei, G. Luo, H. Yu, and G. Gu, "The large-scale production of carbon nanotubes in a nano-agglomerate fluidized-bed reactor," *Chemical Physics Letters*, vol. 364, no. 5-6, pp. 568–572, 2002.

[13] F. Ding, P. Larsson, J. A. Larsson et al., "The importance of strong carbon-metal adhesion for catalytic nucleation of single-walled carbon nanotubes," *Nano Letters*, vol. 8, no. 2, pp. 463–468, 2008.

[14] H. Ago, T. Komatsu, S. Ohshima, Y. Kuriki, and M. Yumura, "Dispersion of metal nanoparticles for aligned carbon nanotube arrays," *Applied Physics Letters*, vol. 77, no. 1, pp. 79–81, 2000.

[15] R. M. Yadav, P. S. Dobal, T. Shripathi, R. S. Katiyar, and O. N. Srivastava, "Effect of growth temperature on bamboo-shaped carbon-nitrogen (C-N) nanotubes synthesized using ferrocene acetonitrile precursor," *Nanoscale Research Letters*, vol. 4, no. 3, pp. 197–203, 2008.

[16] D. Yuan, L. Ding, H. Chu, Y. Feng, T. P. McNicholas, and J. Liu, "Horizontally aligned single-walled carbon nanotube on quartz from a large variety of metal catalysts," *Nano Letters*, vol. 8, no. 8, pp. 2576–2579, 2008.

[17] Y. Alinejad, A. Shahverdi, N. Faucheux, and G. Soucy, "Synthesis of single-walled carbon nanotubes using induction thermal plasma technology with different catalysts: thermodynamic and experimental studies," *Journal of Physics: Conference Series*, vol. 406, article 012019, 2012.

[18] S. L. Pirard, S. Douven, C. Bossuot, G. Heyen, and J.-P. Pirard, "A kinetic study of multi-walled carbon nanotube synthesis by catalytic chemical vapor deposition using a $Fe-Co/Al_2O_3$ catalyst," *Carbon*, vol. 45, no. 6, pp. 1167–1175, 2007.

[19] S. H. Sharif Zein, A. R. Mohamed, and P. S. Talpa Sai, "Kinetic studies on catalytic decomposition of methane to hydrogen and carbon over Ni/TiO_2 catalyst," *Industrial & Engineering Chemistry Research*, vol. 43, no. 16, pp. 4864–4870, 2004.

[20] H. Kathyayini, N. Nagaraju, A. Fonseca, and J. B. Nagy, "Catalytic activity of Fe, Co and Fe/Co supported on Ca and Mg oxides, hydroxides and carbonates in the synthesis of carbon nanotubes," *Journal of Molecular Catalysis A: Chemical*, vol. 223, no. 1-2, pp. 129–136, 2004.

[21] K. Inoue, "Functional dendrimers, hyperbranched and star polymers," *Progress in Polymer Science*, vol. 25, no. 4, pp. 453–571, 2000.

[22] S. Inoue, T. Nakajima, and Y. Kikuchi, "Synthesis of single-wall carbon nanotubes from alcohol using Fe/Co, Mo/Co, Rh/Pd catalysts," *Chemical Physics Letters*, vol. 406, no. 1-3, pp. 184–187, 2005.

[23] S. Shukrullah, N. M. Mohamed, and M. S. Shaharun, "Optimum temperature on structural growth of multiwalled carbon nanotubes with low activation energy," *Diamond and Related Materials*, vol. 58, pp. 129–138, 2015.

[24] S. Shukrullah, N. M. Mohamed, M. S. Shaharun, and M. Y. Naz, "Parametric study on vapor-solid-solid growth mechanism of multiwalled carbon nanotubes," *Materials Chemistry and Physics*, vol. 176, pp. 32–43, 2016.

[25] C. H. See and A. T. Harris, "A Review of carbon nanotube synthesis via fluidized-bed chemical vapor deposition," *Industrial & Engineering Chemistry Research*, vol. 46, no. 4, pp. 997–1012, 2007.

[26] H. M. Cheng, F. Li, X. Sun et al., "Bulk morphology and diameter distribution of single-walled carbon nanotubes synthesized by catalytic decomposition of hydrocarbons," *Chemical Physics Letters*, vol. 289, no. 5-6, pp. 602–610, 1998.

[27] L. Delzeit, C. V. Nguyen, B. Chen et al., "Multiwalled carbon nanotubes by chemical vapor deposition using multilayered metal catalysts," *The Journal of Physical Chemistry B*, vol. 106, no. 22, pp. 5629–5635, 2002.

[28] I. B. Usman, B. Matsoso, K. Ranganathan, D. Naidoo, N. J. Coville, and D. Wamwangi, "Magnetic properties of aligned iron containing nitrogen-doped multi-walled carbon nanotubes," *Materials Chemistry and Physics*, vol. 209, pp. 280–290, 2018.

[29] S. Point, T. Minea, B. Bouchet-Fabre, A. Granier, and G. Turban, "XPS and NEXAFS characterisation of plasma deposited vertically aligned N-doped MWCNT," *Diamond and Related Materials*, vol. 14, no. 3-7, pp. 891–895, 2005.

[30] V. I. Alexiadis, N. Boukos, and X. E. Verykios, "Influence of the composition of Fe_2O_3/Al_2O_3 catalysts on the rate of production and quality of carbon nanotubes," *Materials Chemistry and Physics*, vol. 128, no. 1-2, pp. 96–108, 2011.

[31] V. I. Alexiadis and X. E. Verykios, "Influence of structural and preparation parameters of Fe_2O_3/Al_2O_3 catalysts on rate of production and quality of carbon nanotubes," *Materials Chemistry and Physics*, vol. 117, no. 2-3, pp. 528–535, 2009.

[32] K. B. Kouravelou and S. V. Sotirchos, "Dynamic study of carbon nanotubes production by chemical vapor deposition of alcohols," *Reviews on Advanced Materials Science*, vol. 10, pp. 243–248, 2005.

[33] M. Kumar and Y. Ando, "Chemical vapor deposition of carbon nanotubes: a review on growth mechanism and mass production," *Journal of Nanoscience and Nanotechnology*, vol. 10, no. 6, pp. 3739–3758, 2010.

[34] L. Ni, K. Kuroda, L. P. Zhou et al., "Kinetic study of carbon nanotube synthesis over Mo/Co/MgO catalysts," *Carbon*, vol. 44, no. 11, pp. 2265–2272, 2006.

[35] M. Z. Hussein, A. M. Jaafar, A. H. Yahaya, M. J. Masarudin, and Z. Zainal, "Formation and yield of multi-walled carbon nanotubes synthesized via chemical vapour deposition routes using different metal-based catalysts of FeCoNiAl, CoNiAl and FeNiAl-LDH," *International Journal of Molecular Sciences*, vol. 15, no. 11, pp. 20254–20265, 2014.

[36] S. Shukrullah, M.Y. Naz, N.M. Mohamed, K.A. Ibrahim, A. Ghaffar, and N.M. AbdEl-Salam, "Production of bundled CNTs by floating a compound catalyst in an atmospheric pressure horizontal CVD reactor," *Results in Physics*, vol. 12, pp. 1163–1171, 2019.

[37] A. Abad, F. García-Labiano, L. F. de Diego, P. Gayán, and J. Adánez, "Reduction kinetics of Cu-, Ni-, and Fe-based oxygen carriers using syngas ($CO+H_2$) for chemical-looping combustion," *Energy & Fuels*, vol. 21, no. 4, pp. 1843–1853, 2007.

[38] A. M. Kierzkowska, C. D. Bohn, S. A. Scott, J. P. Cleeton, J. S. Dennis, and C. R. Müller, "Development of iron oxide carriers for chemical looping combustion using sol-gel," *Industrial & Engineering Chemistry Research*, vol. 49, no. 11, pp. 5383–5391, 2010.

[39] N. Nagaraju, A. Fonseca, Z. Konya, and J. B. Nagy, "Alumina and silica supported metal catalysts for the production of carbon nanotubes," *Journal of Molecular Catalysis A: Chemical*, vol. 181, no. 1-2, pp. 57–62, 2002.

[40] H. Ago, K. Nakamura, N. Uehara, and M. Tsuji, "Roles of metal-support interaction in growth of single- and double-walled carbon nanotubes studied with diameter-controlled iron particles supported on MgO," *The Journal of Physical Chemistry B*, vol. 108, no. 49, pp. 18908–18915, 2004.

[41] C. Mattevi, C. T. Wirth, S. Hofmann et al., "In-situ X-ray photoelectron spectroscopy study of catalyst-support interactions and growth of carbon nanotube forests," *The Journal of Physical Chemistry C*, vol. 112, no. 32, pp. 12207–12213, 2008.

[42] S. Noda, K. Hasegawa, H. Sugime et al., "Millimeter-thick single-walled carbon nanotube forests: hidden role of catalyst support," *Japanese Journal of Applied Physics*, vol. 46, no. 17, pp. L399–L401, 2007.

[43] M. Kumar and Y. Ando, "Gigas growth of carbon nanotubes," *Defence Science Journal*, vol. 58, no. 4, pp. 496–503, 2008.

[44] W. Zhao, H. S. Kim, H. T. Kim, J. Gong, and I. J. Kim, "Synthesis and growth of multi-walled carbon nanotubes (MWNTs) by CCVD using Fe-supported zeolite templates," *Journal of Ceramic Processing Research*, vol. 12, pp. 392–397, 2011.

[45] J. P. Tessonnier and D. S. Su, "Recent progress on the growth mechanism of carbon nanotubes: a review," *ChemSusChem*, vol. 4, no. 7, pp. 824–847, 2011.

[46] M. Kumar and Y. Ando, "Controlling the diameter distribution of carbon nanotubes grown from camphor on a zeolite support," *Carbon*, vol. 43, no. 3, pp. 533–540, 2005.

[47] M. Kumar and Y. Ando, "Camphor—a botanical precursor producing garden of carbon nanotubes," *Diamond and Related Materials*, vol. 12, no. 3-7, pp. 998–1002, 2003.

[48] A. A. Muataz, F. Ahmadun, C. Guan, E. Mahdi, and A. Rinaldi, "Effect of reaction temperature on the production of carbon nanotubes," *Nano*, vol. 1, no. 3, pp. 251–257, 2006.

[49] X. Fu, X. Cui, X. Wei, and J. Ma, "Investigation of low and mild temperature for synthesis of high quality carbon nanotubes by chemical vapor deposition," *Applied Surface Science*, vol. 292, pp. 645–649, 2014.

[50] W. Qian, T. Liu, F. Wei, Z. Wang, and Y. Li, "Enhanced production of carbon nanotubes: combination of catalyst reduction and methane decomposition," *Applied Catalysis A: General*, vol. 258, no. 1, pp. 121–124, 2004.

[51] J.-l. Song, L. Wang, S.-a. Feng, J.-h. Zhao, and Z.-p. Zhu, "Growth of carbon nanotubes by the catalytic decomposition of methane over Fe-Mo/Al_2O_3 catalyst: effect of temperature on tube structure," *New Carbon Materials*, vol. 24, no. 4, pp. 307–313, 2009.

[52] O. V. Kharissova and B. I. Kharisov, "Variations of interlayer spacing in carbon nanotubes," *RSC Advances*, vol. 4, no. 58, pp. 30807–30815, 2014.

[53] Y. Liu, W. Z. Qian, Q. Zhang et al., "Synthesis of high-quality, double-walled carbon nanotubes in a fluidized bed reactor," *Chemical Engineering & Technology*, vol. 32, no. 1, pp. 73–79, 2009.

[54] C.-M. Chen, Y.-M. Dai, J. G. Huang, and J.-M. Jehng, "Intermetallic catalyst for carbon nanotubes (CNTs) growth by thermal chemical vapor deposition method," *Carbon*, vol. 44, no. 9, pp. 1808–1820, 2006.

The Scientific
World Journal

Journal of
Applied Chemistry

Journal of
Nanomaterials

Scientifica

International Journal of
Polymer Science

Advances in
Chemistry

Advances in
Physical Chemistry

International Journal of
Analytical Chemistry

Hindawi

Submit your manuscripts at
www.hindawi.com

Advances in
Condensed Matter Physics

Journal of
Chemistry

International Journal of
Biomaterials

Advances in
High Energy Physics

Journal of
Engineering

Journal of
Nanotechnology

International Journal of
Corrosion

Journal of
Materials

BioMed
Research International

Advances in
Tribology

Advances in
Materials Science and Engineering